Sodium is a negative allosteric regulator of the ghrelin receptor

Guillaume Ferré, Antoniel A.S. Gomes, Maxime Louet, Marjorie Damian, Paulo Bisch, Olivier Saurel, Nicolas Floquet, Alain Milon, Jean-Louis Banères

Cell Reports

Sodium is a negative allosteric regulator of the ghrelin receptor

Graphical abstract

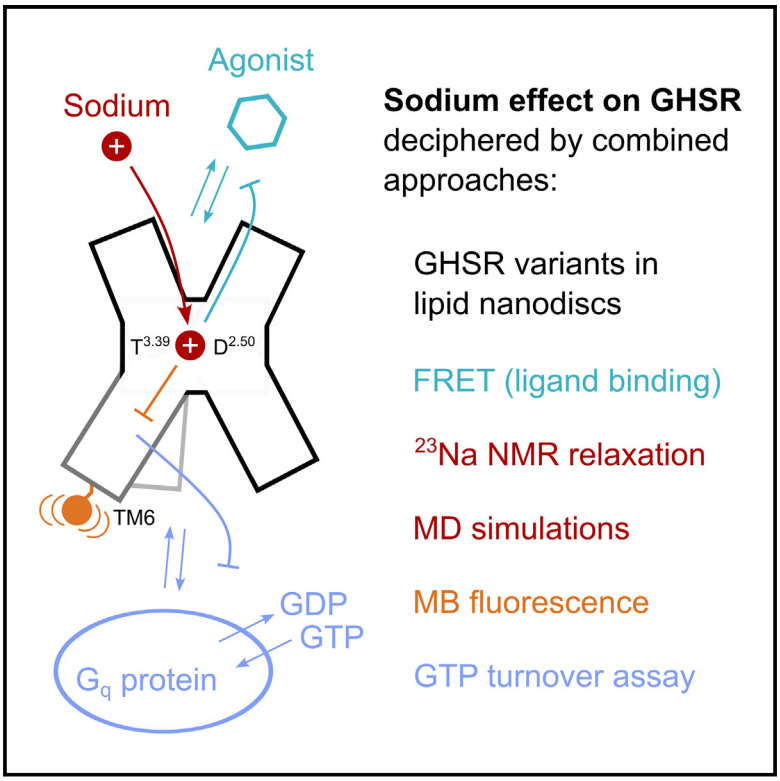

Authors

Guillaume Ferré, Antoniel A.S. Gomes, Maxime Louet, ..., Nicolas Floquet, Alain Milon, Jean-Louis Banères

Correspondence

alain.milon@ipbs.fr (A.M.), jean-louis.baneres@umontpellier.fr (J.-L.B.)

In brief

Sodium is one of the most abundant ions in the body. Here, Ferré et al. provide evidence that this ion binds the ghrelin receptor and, by doing so, negatively impacts its signaling properties through an allosteric mechanism. As such, sodium could be a central player in ghrelin signaling.

Highlights

- The ghrelin receptor binds sodium ions at its allosteric site
- Sodium binding favors the receptor inactive/inactive-like conformational ensemble
- Sodium binding decreases agonist affinity and receptor-catalyzed G protein activation

Ferré et al., 2023, Cell Reports *42*, 112320
April 25, 2023
https://doi.org/10.1016/j.celrep.2023.112320

Cell Reports

CellPress
OPEN ACCESS

Report

Sodium is a negative allosteric regulator of the ghrelin receptor

Guillaume Ferré,[1] Antoniel A.S. Gomes,[2,3] Maxime Louet,[2] Marjorie Damian,[2] Paulo M. Bisch,[3] Olivier Saurel,[1] Nicolas Floquet,[2] Alain Milon,[1,*] and Jean-Louis Banères[2,4,*]

[1]Institut de Pharmacologie et de Biologie Structurale IPBS, Université de Toulouse UPS, CNRS, Toulouse, France
[2]Institut des Biomolécules Max Mousseron IBMM, UMR-5247, University Montpellier, CNRS, ENSCM, Montpellier, France
[3]Laboratório de Física Biológica, Instituto de Biofísica Carlos Chagas Filho, Universidade Federal do Rio de Janeiro, Rio de Janeiro 21941-590, Brazil
[4]Lead contact
*Correspondence: alain.milon@ipbs.fr (A.M.), jean-louis.baneres@umontpellier.fr (J.-L.B.)
https://doi.org/10.1016/j.celrep.2023.112320

SUMMARY

The functional properties of G protein-coupled receptors (GPCRs) are intimately associated with the different components in their cellular environment. Among them, sodium ions have been proposed to play a substantial role as endogenous allosteric modulators of GPCR-mediated signaling. However, this sodium effect and the underlying mechanisms are still unclear for most GPCRs. Here, we identified sodium as a negative allosteric modulator of the ghrelin receptor GHSR (growth hormone secretagogue receptor). Combining ^{23}Na-nuclear magnetic resonance (NMR), molecular dynamics, and mutagenesis, we provide evidence that, in GHSR, sodium binds to the allosteric site conserved in class A GPCRs. We further leveraged spectroscopic and functional assays to show that sodium binding shifts the conformational equilibrium toward the GHSR-inactive ensemble, thereby decreasing basal and agonist-induced receptor-catalyzed G protein activation. All together, these data point to sodium as an allosteric modulator of GHSR, making this ion an integral component of the ghrelin signaling machinery.

INTRODUCTION

G protein-coupled receptors (GPCRs) are major players in most cell communication events.[1] Experimental and computational strategies aimed at exploring receptor dynamics point to a model where the control of signaling relies on the conformational plasticity of GPCRs.[2,3] In this model, receptors explore complex energy landscapes populated by multiple conformational states with distinct functional properties with respect to their downstream effectors. Beside orthosteric ligands, endogenous allosteric modulators—lipids, ions, oligomerization partners, intracellular proteins—regulate the distribution of the different states in the conformational ensemble and, as a consequence, the final signaling output.[4]

Sodium is one of the most abundant ions in the human body, where concentration is dynamically regulated.[5] Sodium is essential for cell energetics, homeostasis, neural function, and many other crucial physiological processes.[5] From the early stages of GPCR pharmacology, this ion has been identified as a negative allosteric modulator of agonist binding to opioid receptors.[6] Since then, the role of sodium has been shown to be more general and to affect the pharmacological profile of several GPCRs.[7] High-resolution crystal structures of class A GPCRs and mutagenesis studies have provided a molecular basis to these observations by revealing the occurrence of a binding site where highly conserved residues—D2x50 (GPCRdb numbering[8]), S/T3x39, W6x48, and N7x49—coordinate sodium.[9] Sodium binding to this site was further proposed to stabilize the receptor inactive conformation.[10] Based on these observations, a model was proposed to account for the impact of sodium ions on GPCR activation.[11] In this model, Na^+ would enter from the solvent in the extracellular part of the receptor, bind the allosteric site, and, by doing so, stabilize the receptor inactive state, thereby decreasing receptor basal activity. Upon agonist binding, the sodium-binding site would collapse, promoting a directional Na^+ release into the cytoplasm because of both the membrane potential and a sodium concentration gradient. As such, Na^+ transfer would participate in agonist-dependent receptor activation.

Here, we investigated the role of sodium ions in modulating the activity of the ghrelin receptor. Ghrelin is a gastrointestinal peptide hormone that exerts a wide range of biological effects through a single class A GPCR, the growth hormone secretagogue receptor (GHSR).[12] To the best of our knowledge, regulation of functional and structural dynamics by sodium has never been demonstrated for GHSR. In contrast to other GPCRs, sodium is not observed in the crystal structure of the antagonist-bound GHSR.[13] However, this is certainly due to the fact that one of the conserved potential sodium-binding residues, T130$^{3.39}$ (superscript indicates Ballesteros and Weinstein numbering[14]), was mutated to increase receptor stability for crystallization purposes. Here, we used a combination of experimental and computational methods to investigate potential interactions of GHSR with sodium and their

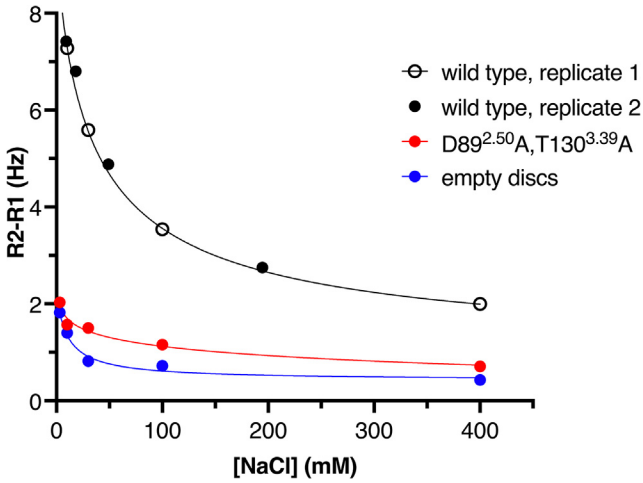

Figure 1. Sodium binding to GHSR as probed by ^{23}Na-NMR

Relaxation rates of ^{23}Na, R_2-R_1, as a function of NaCl concentration for the apo wild-type GHSR (two replicates) and its D89$^{2.50}$A, T130$^{3.39}$A double mutant. Empty MSP1E3D1:POPC:POPG nanodiscs were used as a negative control.

consequences on receptor conformational dynamics and pharmacological properties. We demonstrated that sodium ions bind to the receptor isolated in lipid nanodiscs and that this binding is abrogated by mutations in the canonical sodium-binding site. Sodium binding is accompanied by a modulation of the receptor conformational equilibria and, thereby, of its efficacy at activating G proteins. Altogether, this provides direct evidence for sodium binding and how it impacts the conformational ensemble of GHSR isolated in a lipid environment as a representative member of the β-branch of rhodopsin-like GPCRs in which sodium effects are much less studied.

RESULTS

Sodium binding to GHSR

We first examined sodium binding *in vitro* using ^{23}Na-nuclear magnetic resonance (NMR) with monomeric GHSR purified and inserted into lipid nanodiscs. This method allows a direct assessment of sodium binding by measuring the relaxation rates (R_2 and R_1) as a function of ion concentration (see STAR Methods). A major issue in these experiments is the potential contribution from non-specific binding events, as the typical K_d value for the GPCR sodium-binding sites is high and may be close to the non-specific binding constants for lipid surfaces (Figure S1). We thus developed a workflow to suppress these undesired contributions and quantitatively assess sodium binding (see STAR Methods). In particular, we used nanodiscs with less negatively charged lipids compared with our previous work (POPC:POPG molar ratio of 4:1 instead of 3:2). Besides, the NMR measurements were carried out in a buffer at high ionic strength yet essentially devoid of sodium or potassium ions (HEPES/tri-ethyl ammonium [TEA]). TEA is a bulky organic cation that has little chance to compete with sodium for its binding site. As shown in Figure 1, we measured a negligible effect of non-specific binding to empty nanodiscs under such conditions.

We then titrated the apo receptor in lipid nanodiscs with increasing amounts of sodium chloride and measured the sodium R_2 and R_1 relaxation rates for each concentration. Fitting R_2-R_1 as a function of sodium chloride concentration by a single-site binding equation (see STAR Methods) provided a K_d value of 43.5 ± 10.7 mM (Figure 1). These data show that sodium binds to GHSR, in a transient but specific manner, with a dissociation constant in the 40 mM range.

We then combined site-directed mutagenesis with ^{23}Na-NMR to assess whether the canonical site found in class A GPCRs could also be responsible for Na^+ binding to GHSR. A stated above, this canonical site is formed by the highly conserved residues D2x50, S/T3x39, W6x48, and N7x49.[9] W276$^{6.48}$ could not be mutated in GHSR because replacing this highly conserved tryptophan significantly decreased both constitutive and agonist-induced G protein activation (Figure S2), in agreement with previous reports in the literature.[15,16] This indicates that this substitution likely affects the fold and/or the activation mechanism of GHSR, consistent with the central role of W276$^{6.48}$ in GHSR activation.[17] As such, it would render any effect on sodium binding inconclusive. To be noted, W276$^{6.48}$ was substituted here by an Ala, as this mutation had been already described in the literature, but other substitutions have been shown to lead to a similar phenotype.[15] N319$^{7.49}$ could not be modified either, as replacing it with an Ala abolished the ability of the isolated receptor to activate its cognate G protein both in an agonist-independent and -dependent manner (Figure S2). This is in line with the fact that this residue belongs to the conserved NPxxY motif, a motif that has been shown to be directly involved in GHSR activation and coupling to G proteins.[17] Hence, we mutated D89$^{2.50}$ and T130$^{3.39}$ only to alanines. The resulting D89$^{2.50}$A, T130$^{3.39}$A mutant of GHSR was functional with regard to Gq activation and conformational equilibria (see below). We then titrated the mutant apo receptor in lipid nanodiscs with increasing amounts of sodium under the same conditions as those used for the wild type GHSR. As shown in Figure 1, essentially no binding of Na^+ was observed with the D89$^{2.50}$A, T130$^{3.39}$A mutant when measuring the sodium R_2 and R_1 relaxation rates for each concentration. As the ^{23}Na-NMR experiments do not directly show where sodium binds, we cannot exclude at this stage an allosteric effect of the mutations that would indirectly affect sodium binding. This result nevertheless strongly points to D89$^{2.50}$ and T130$^{3.39}$ as central components of sodium binding in GHSR, indicating that the conserved Na^+-binding site is also certainly present in GHSR and could be responsible for sodium binding to this receptor. To be noted, by offering to sodium ions the same environment for non-specific binding, the D89$^{2.50}$A, T130$^{3.39}$A double mutant also provides a good negative control to ensure that the R_2 relaxation rate changes observed with the wild-type receptor were indeed due to specific binding events.

Sodium-binding pathway

To get a three-dimensional framework for sodium binding to GHSR, we then analyzed this process *in silico* using all-atom molecular dynamics (MD) simulations, starting from the crystal structure of GHSR in its antagonist-bound state.[13] For these simulations, the T130$^{3.39}$K mutation introduced in the construct

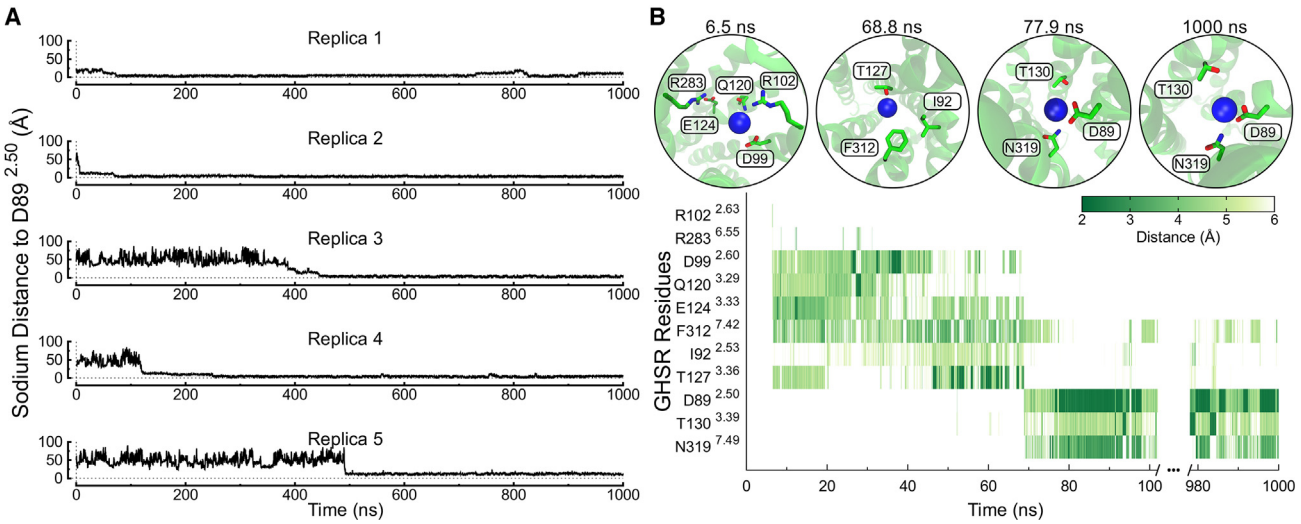

Figure 2. Sodium binding to GHSR

(A) Graphical representation for each MD simulation of the computed distance between Na^+ ions and $D89^{2.50}$ of GHSR . The dotted line corresponds to zero values for both x and y axes.

(B) Temporal description of the participation of GHSR residues to sodium binding for one replica (see Figure S3 for the other replicas). The distance of a residue to sodium was determined by the minimal distance of their non-hydrogen atoms to the ion. Distances are shown as different tonalities of green, with close proximity shown in dark green and larger distances in light green.

used for crystallization was reverted, as the ^{23}Na-NMR data indicate that this residue likely participates in ion binding, consistent with its role as part of the conserved sodium site in class A GPCRs (Figure S3A). As a control, equivalent MD simulations were performed on the dopamine receptor D2R (Figure S3B), where sodium had been shown to bind.[18] The root-mean-square deviation (RMSD) curves show that a stable conformation was reached in each replica for both receptors during several hundreds of nanoseconds (Figure S3C). Consistent with the ^{23}Na-NMR data, the MD simulations showed spontaneous binding of sodium to its allosteric site in GHSR, close to $D89^{2.50}$, in four out of five simulations (Figure 2). Such a binding always occurred from the extracellular side of the receptor (see Video S1). In one of the simulations, however, sodium stabilized in an upper position, at a distance of 12 Å from $D89^{2.50}$ (Figure 2A).

To better understand how Na^+ transits from the bulk to its allosteric site in GHSR, we analyzed its interactions with the receptor residues as a function of time. As shown in Figure 2B (see Figure S3D for all replicas), the sodium ion made a pause in the orthosteric site of the receptor, establishing contacts with several residues that are involved in ghrelin binding (e.g., $D99^{2.60}$, $Q120^{3.29}$, $E124^{3.33}$),[17] and lying, with marginal frequency, close to $R102^{2.63}$ and $R283^{6.55}$, two residues that are also part of the ghrelin-binding pocket.[17] After this first step, Na^+ shifted deeper into the receptor to reach its final position close to residues $D89^{2.50}$, $T130^{3.39}$, and $N319^{7.49}$. The observation that $D89^{2.50}$ and $T130^{3.39}$ would participate in sodium binding is fully consistent with our NMR and mutagenesis data. Once bound, the sodium ion kept its position in all replicas and had the same interaction pattern with GHSR, except in replica 1, along which we observed two unbinding events around 725 and 925 ns. To be noted, the transition between the orthosteric and allosteric sites appeared to be less frequent with GHSR than with the control receptor, D2R (Figure S3), thereby slowing down the binding events of sodium into its allosteric site. This could be related to the presence of hydrophobic residues, in particular $F312^{7.42}$, along the sodium-binding pathway in GHSR, as in D2R, a glycine occupies the same position. Indeed, the occurrence of a hydrophobic barrier has been proposed to control the egress of Na^+ to its allosteric site (see discussion).[19]

Sodium binding impacts receptor and G protein activation

To assess whether sodium binding to GHSR was accompanied by a change in the receptor pharmacological profile, we then investigated the agonist-binding properties of the isolated receptor in the absence or presence of sodium ions. As shown in Figure 3A, Na^+ affected the binding of ghrelin to the isolated receptor in nanodiscs. Namely, GHSR displayed a ca. 8-fold lower affinity for the labeled ghrelin peptide in the presence of NaCl, consistent with previous results in the literature showing that sodium decreases the affinity of GPCRs for their agonist.[7] Although, as stated above, an allosteric effect of the mutations cannot be excluded, this is nevertheless likely the result of sodium binding to its allosteric site, as the $D89^{2.50}$A, $T130^{3.39}$A double mutant bound ghrelin with essentially the same high affinity whether Na^+ was present or not (Figure 3B). To be noted, no major effect of sodium on ghrelin binding was observed with the $D89^{2.50}$A and $T130^{3.39}$A single mutants either, at least in the NaCl concentration range we used (Figure S4A). This indicates each of these residues is likely central to sodium binding.

We then investigated G protein activation by GHSR in lipid nanodiscs in the absence or the presence of sodium ions. Without sodium, apo GHSR triggered a significant GTP turnover

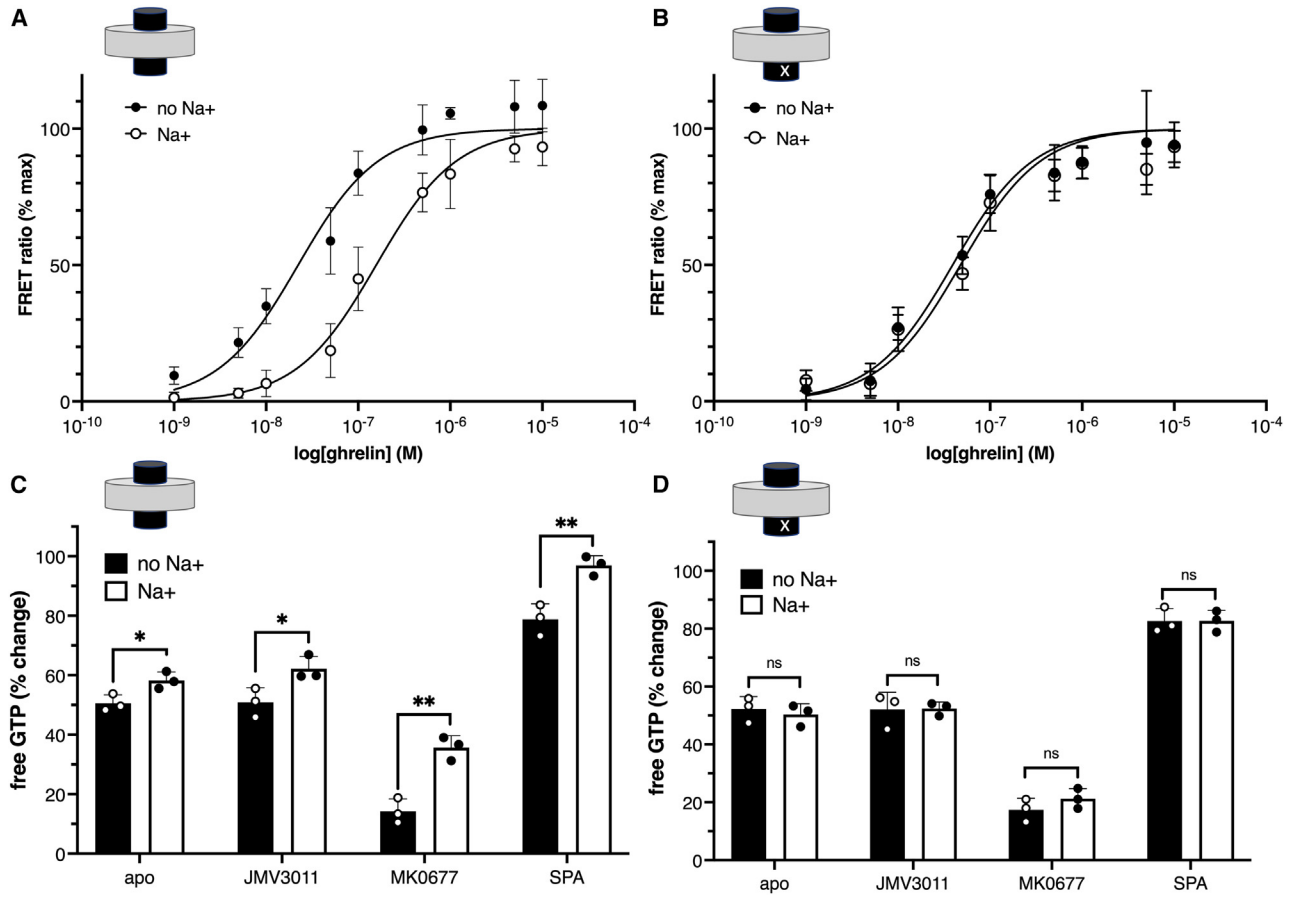

Figure 3. Sodium binding affects receptor pharmacological profile

(A and B) Fluorescence resonance energy transfer (FRET)-monitored ghrelin binding to wild-type GHSR (A) or to its D89$^{2.50}$A, T130$^{3.39}$A double mutant (B) in the absence or presence of 250 mM Na^+.

(C and D) GTP turnover for Gq-catalyzed by wild-type GHSR (C) or its D89$^{2.50}$A, T130$^{3.39}$A double mutant (D) in the absence or presence of 250 mM Na^+ and in the absence of ligand or in the presence of 10 μM JMV3011 (neutral antagonist), MK0677 (full agonist), or SPA (inverse agonist). The signal was normalized to that obtained for the isolated G protein in the presence of empty nanodiscs.

In all cases, data are mean ± SD of three experiments. Statistical values were obtained by means of unpaired Student's t test (*0.01 < p < 0.05, **0.001 < p < 0.01).

on the Gq protein, in agreement with its constitutive activity in the Gq pathway. The full agonist MK0677 increased GTP turnover, as indicated by the decrease in free GTP, whereas the inverse agonist SPA decreased GTP turnover (Figure 3C). The neutral antagonist JMV3011 had no impact on basal GTP turnover (Figure 3C). In all cases, the presence of sodium was associated with a decrease in GTP turnover (Figure 3C), with a larger amplitude for the agonist-stimulated effect. In contrast, no significant impact of sodium was observed for the D89$^{2.50}$A, T130$^{3.39}$A double mutant (Figure 3D), indicating that the effect of sodium on GTP turnover could result from its binding to the receptor. In the same way, no major effect was observed with the D89$^{2.50}$A and T130$^{3.39}$A single mutants (Figure S4B). Altogether, these results indicate that binding of sodium to GHSR allosterically decreases its efficacy at activating Gq.

To further illuminate the mechanism involved in the effect of sodium binding on GHSR functioning, we explored the impact of this ion on the conformational features of the isolated receptor in lipid nanodiscs using monobromobimane (MB) fluorescence spectroscopy. To this end, MB was attached to C255$^{6.27}$ in the cytoplasmic end of TM6. When MB is located at this position, changes in its emission properties primarily report on the movements of TM6 associated with receptor activation.[20] In the absence of sodium, the binding of the full agonist MK0677 was associated with a significant change in MB emission, with a decrease in the emission intensity and a redshift in the maximum emission wavelength λ_{max} (Figures 4A and 4B). In the presence of sodium, the change in maximum emission intensity and wavelength was of lower amplitude, both in the absence of ligand and in the presence of MK0677 (Figures 4A and 4B). As in the case of GTP turnover, the effect was of significantly lower amplitude in the absence of ligand than in the presence of MK0677. In contrast, no relevant effect was observed with the D89$^{2.50}$A, T130$^{3.39}$A double mutant (Figure 4B) nor with the D89$^{2.50}$A and T130$^{3.39}$A single mutants (Figure S4C). Altogether, these data suggest that sodium allosterically shifts the equilibrium away from the agonist-stabilized active state of GHSR and toward its inactive conformational ensemble.

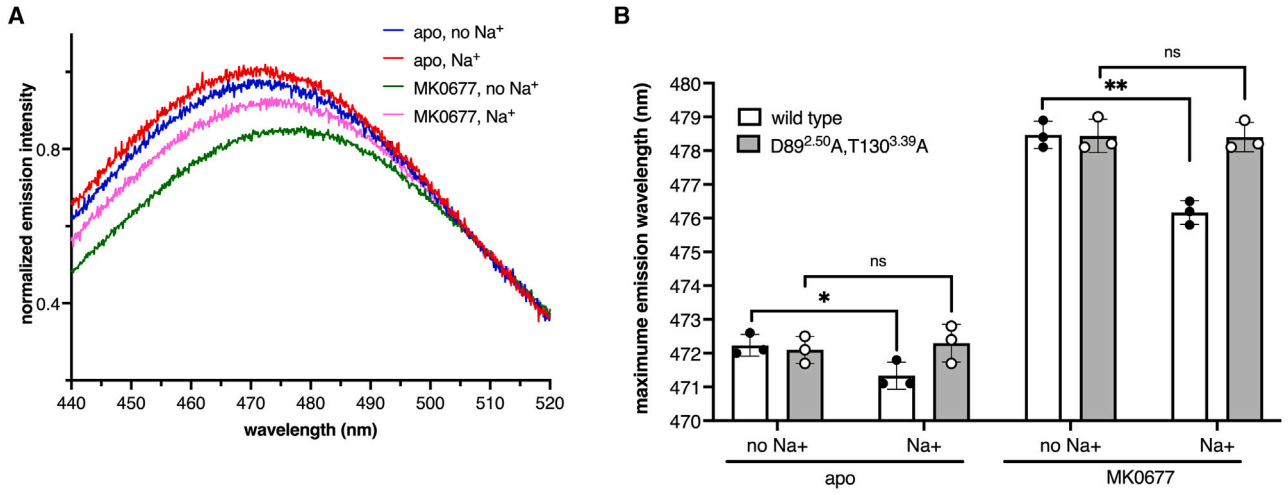

Figure 4. Sodium binding affects receptor conformation

(A) MB emission spectra of GHSR in the absence or presence of 250 mM Na^+, in the absence of ligand, or in the presence of 10 μM MK0677. The spectra were normalized to that of the apo receptor in the presence of sodium.

(B) Changes in λ_{max} inferred from the MB emission spectra.

Data in (B) are mean ± SD of three experiments. Statistical values were obtained by means of unpaired Student's t test (*0.01 < p < 0.05, **0.001 < p < 0.01).

DISCUSSION

Combining ^{23}Na-NMR, fluorescence measurements, functional assays, and MD, we demonstrated here that sodium ions could act as negative allosteric modulators of the ghrelin receptor. Specifically, our data suggest a mechanism where sodium would bind to the conserved allosteric site in the ghrelin receptor through a well-defined pathway and, by doing so, would limit excursions to the receptor active state, thereby decreasing its ability to catalyze G protein activation.

^{23}Na-NMR has long been used to characterize sodium binding to biomolecules and to determine dissociation constants in the 10 to 100 mM range.[21] However, to the best of our knowledge, it has been used only once with GPCRs, in a study demonstrating sodium binding to solubilized A_{2A}AR in LMNG-CHS micelles.[10] Using this method, we demonstrated here that GHSR in lipid nanodiscs binds sodium with an affinity in the 40 mM range, a value close to that reported for A_{2A}AR in the above-mentioned analyses. K_d values in a similar range were also indirectly inferred from the effect of Na^+ on the functional properties of several other class A GPCRs.[7] To be noted, such an affinity value could lead to transiently sodium-occupied states if the on rate is diffusion limited. In this respect, an average residence time for Na^+ of 480 μs was reported for the ligand-free A_2AR in detergent micelles.[10] However, the on rate of sodium binding is likely to be influenced by different features in the cell environment such as the concentration gradient and membrane potential,[11] all features nanodiscs and detergents do not recapitulate.

Besides pointing at the residues that might be involved in sodium binding, the all-atom simulations delineate the possible sodium-binding pathway and suggest a particular role for hydrophobic residues along this pathway in the egress of sodium to its allosteric site. The exact role of these residues is still to be assessed, however, as sodium access is also likely influenced by dynamic fluctuations of the protonation states of Asp, Glu, His, and Gln residues along the binding pathway. However, this is reminiscent of a recent analysis of Na^+ interaction with conserved orthosteric and allosteric residues in multiple GPCR simulations that led to the classification of the receptors into three different groups depending on their sodium-binding behavior.[19] The first one shows high sodium interaction frequencies with both the allosteric and orthosteric site. The second one shows marginal interaction frequency with Dx2.50 because of a hydrophobic barrier that hampers Na^+ passage from the orthosteric to the allosteric site. In the last group, Na^+ shows no or few contacts with the residues in the allosteric site. Based on these considerations, GHSR could fall into group II.

In addition to directly demonstrate the binding of sodium ions to GHSR, our data indicate that such binding is accompanied by a decrease in the affinity for the agonist and a negative effect on receptor-catalyzed G protein activation, probably because of a smaller shift of the conformational equilibrium toward the active state of GHSR when sodium is bound. Hence, a possible mechanism would be that bound sodium prevents excursions to the agonist-activated state and/or decreases the time the receptor spends in this activated state, thereby playing the role of a negative allosteric modulator of ghrelin-dependent GHSR activation. A similar conclusion was reached from ^{19}F-NMR measurements with the isolated A_{2A}AR in detergent micelles. Indeed, the addition of sodium to the apo receptor shifted the equilibrium toward the inactive conformational ensemble of A_{2A}AR at the expense of the active one.[10] To be noted, both agonist-stimulated and constitutive G protein activation were affected here by Na^+ binding. This is in contrast to several results in the literature reporting that the presence of sodium reduces the basal activity of GPCRs but enhances agonist-stimulated responses.[7] A mechanism has been proposed to explain this behavior that relies on the

occurrence of a sodium gradient concentration and a membrane potential.[11] In this model, the movements of the transmembrane domains associated with agonist-induced receptor activation would lead to sodium release from its site. Because of this ion concentration gradient and membrane electrostatic potential, unbound sodium would exclusively exit toward the cytoplasmic compartment. This transmembrane transfer of sodium would lower the energy barrier for receptor activation and thus facilitate agonist-induced signaling. This directional Na^+ displacement would also affect the protonation state of Dx2.50, which could also impact on receptor activation.[22] Although it cannot be excluded that the decrease in agonist-induced G protein activation upon Na^+ binding we observe with GHSR is a particular feature of this receptor, an alternative, possible explanation could nevertheless be related to the fact that there is no compartmentalization, and therefore no possible concentration gradient, when using nanodiscs instead of a cell-based system. In addition, the membrane in these discs is neither polarized nor asymmetric. Taken together, this could blunt the impact of the directional ion transfer, revealing only the direct effect of sodium binding on the GHSR conformational ensemble.

In closing, our observations raise the question of whether ghrelin receptor activation and sodium translocation are coupled processes with a physiological impact. GPCRs are subject to spatiotemporal changes in the salt concentration of their immediate environment, and this may therefore impact on their signaling properties. Besides, the K_d value of sodium binding to GHSR is in the same range as the physiological sodium concentrations.[5] Hence, any change in the local sodium concentration could change the binding status of Na^+ ions and consequently both the basal activity of GHSR and its response to ghrelin binding. In this model, sodium ions would therefore be an integral part of the allosteric network responsible for ghrelin signaling regulation.

Limitations of the study

These studies were carried out with a purified receptor isolated in an open model membrane system, lipid nanodiscs. As such, they recapitulate the direct effects of sodium binding on GHSR molecular features but do not take into account the impact of some specific features of the cellular environment such as compartmentalization, membrane potential, and bilayer asymmetry that all are to modulate the effect of Na^+ on signaling.

STAR★METHODS

Detailed methods are provided in the online version of this paper and include the following:

SUPPLEMENTAL INFORMATION

Supplemental information can be found online at https://doi.org/10.1016/j.celrep.2023.112320.

ACKNOWLEDGMENTS

We thank Julie Kniazeff (IBMM, Montpellier) for a critical reading of the manuscript and for very fruitful discussions. This work was supported by CNRS, Université de Montpellier, Université de Toulouse UPS, the Agence Nationale de la Recherche (ANR-17-CE11-0011, ANR-17-CE17-0022, and ANR-20-CE92-0028), and the Fondation pour la Recherche Médicale (Équipe FRM EQ202103012736). We thank CAMPUS FRANCE for promoting the French-Brazilian collaboration via CAPES-COFECUB project number Ph-C882/17. We also thank GENCI (Grand Équipement National de Calcul Intensif) and TGCC/IDRIS for having selected us for the "Great Challenge" phases of both the IRENE JOLIOT-CURIE and JEAN-ZAY supercomputers.

AUTHOR CONTRIBUTIONS

J.-L.B., A.M., and N.F. conceived and designed the experiments. G.F., A.A.S.G., M.L., M.D., and O.S. performed the experiments. All authors analyzed the data. J.-L.B. wrote the paper with input from all other authors.

DECLARATION OF INTERESTS

The authors declare no competing interests.

Received: April 19, 2022
Revised: November 9, 2022
Accepted: March 14, 2023
Published: April 5, 2023

REFERENCES

1. Lagerström, M.C., and Schiöth, H.B. (2008). Structural diversity of G protein-coupled receptors and significance for drug discovery. Nat. Rev. Drug Discov. *7*, 339–357. https://doi.org/10.1038/nrd2518.
2. Hilger, D., Masureel, M., and Kobilka, B.K. (2018). Structure and dynamics of GPCR signaling complexes. Nat. Struct. Mol. Biol. *25*, 4–12. https://doi.org/10.1038/s41594-017-0011-7.
3. Wingler, L.M., and Lefkowitz, R.J. (2020). Conformational basis of G protein-coupled receptor signaling versatility. Trends Cell Biol. *30*, 736–747. https://doi.org/10.1016/j.tcb.2020.06.002.
4. Changeux, J.-P., and Christopoulos, A. (2016). Allosteric modulation as a unifying mechanism for receptor function and regulation. Cell *166*, 1084–1102. https://doi.org/10.1016/j.cell.2016.08.015.
5. Bie, P. (2018). Mechanisms of sodium balance: total body sodium, surrogate variables, and renal sodium excretion. Am. J. Physiol. Regul. Integr. Comp. Physiol. *315*, R945–R962. https://doi.org/10.1152/ajpregu.00363.2017.
6. Pert, C.B., Pasternak, G., and Snyder, S.H. (1973). Opiate agonists and antagonists discriminated by receptor binding in brain. Science *182*, 1359–1361. https://doi.org/10.1126/science.182.4119.1359.
7. Zarzycka, B., Zaidi, S.A., Roth, B.L., and Katritch, V. (2019). Harnessing ion-binding sites for GPCR pharmacology. Pharmacol. Rev. *71*, 571–595. https://doi.org/10.1124/pr.119.017863.

8. Kooistra, A.J., Mordalski, S., Pándy-Szekeres, G., Esguerra, M., Mamyrbekov, A., Munk, C., Keserű, G.M., and Gloriam, D.E. (2021). GPCRdb in 2021: integrating GPCR sequence, structure and function. Nucleic Acids Res. *49*, D335–D343. https://doi.org/10.1093/nar/gkaa1080.

9. Liu, W., Chun, E., Thompson, A.A., Chubukov, P., Xu, F., Katritch, V., Han, G.W., Roth, C.B., Heitman, L.H., Ijzerman, A.P., et al. (2012). Structural basis for allosteric regulation of GPCRs by sodium ions. Science *337*, 232–236. https://doi.org/10.1126/science.1219218.

10. Ye, L., Neale, C., Sljoka, A., Lyda, B., Pichugin, D., Tsuchimura, N., Larda, S.T., Pomès, R., García, A.E., Ernst, O.P., et al. (2018). Mechanistic insights into allosteric regulation of the A2A adenosine G protein-coupled receptor by physiological cations. Nat. Commun. *9*, 1372. https://doi.org/10.1038/s41467-018-03314-9.

11. Katritch, V., Fenalti, G., Abola, E.E., Roth, B.L., Cherezov, V., and Stevens, R.C. (2014). Allosteric sodium in class A GPCR signaling. Trends Biochem. Sci. *39*, 233–244. https://doi.org/10.1016/j.tibs.2014.03.002.

12. Müller, T.D., Nogueiras, R., Andermann, M.L., Andrews, Z.B., Anker, S.D., Argente, J., Batterham, R.L., Benoit, S.C., Bowers, C.Y., Broglio, F., et al. (2015). Ghrelin. Mol. Metab. *4*, 437–460. https://doi.org/10.1016/j.molmet.2015.03.005.

13. Shiimura, Y., Horita, S., Hamamoto, A., Asada, H., Hirata, K., Tanaka, M., Mori, K., Uemura, T., Kobayashi, T., Iwata, S., and Kojima, M. (2020). Structure of an antagonist-bound ghrelin receptor reveals possible ghrelin recognition mode. Nat. Commun. *11*, 4160. https://doi.org/10.1038/s41467-020-17554-1.

14. Ballesteros, J.A., and Weinstein, H. (1995). Integrated methods for the construction of three-dimensional models and computational probing of structure-function relations in G protein-coupled receptors. Methods Neurosci. *25*, 366–428. https://doi.org/10.1016/S1043-9471(05)80049-7.

15. Holst, B., Frimurer, T.M., Mokrosinski, J., Halkjaer, T., Cullberg, K.B., Underwood, C.R., and Schwartz, T.W. (2009). Overlapping binding site for the endogenous agonist, small-molecule agonists, and ago-allosteric modulators on the ghrelin receptor. Mol. Pharmacol. *75*, 44–59. https://doi.org/10.1124/mol.108.049189.

16. Gozé, C., Bergé, G., M'Kadmi, C., Floquet, N., Gagne, D., Galleyrand, J.-C., Fehrentz, J.-A., and Martinez, J. (2010). Involvement of tryptophan W276 and of two surrounding amino acid residues in the high constitutive activity of the ghrelin receptor GHS-R1a. Eur. J. Pharmacol. *643*, 153–161. https://doi.org/10.1016/j.ejphar.2010.06.018.

17. Liu, H., Sun, D., Myasnikov, A., Damian, M., Banères, J.-L., Sun, J., and Zhang, C. (2021). Structural basis of human ghrelin receptor signaling by ghrelin and the synthetic agonist ibutamoren. Nat. Commun. *12*, 6410. https://doi.org/10.1038/s41467-021-26735-5.

18. Michino, M., Free, R.B., Doyle, T.B., Sibley, D.R., and Shi, L. (2015). Structural basis for Na(+)-sensitivity in dopamine D2 and D3 receptors. Chem. Commun. *51*, 8618–8621. https://doi.org/10.1039/c5cc02204e.

19. Rodríguez-Espigares, I., Torrens-Fontanals, M., Tiemann, J.K.S., Aranda-García, D., Ramírez-Anguita, J.M., Stepniewski, T.M., Worp, N., Varela-Rial, A., Morales-Pastor, A., Medel-Lacruz, B., et al. (2020). GPCRmd uncovers the dynamics of the 3D-GPCRome. Nat. Methods *17*, 777–787. https://doi.org/10.1038/s41592-020-0884-y.

20. Damian, M., Louet, M., Gomes, A.A.S., M'Kadmi, C., Denoyelle, S., Cantel, S., Mary, S., Bisch, P.M., Fehrentz, J.-A., Catoire, L.J., et al. (2021). Allosteric modulation of ghrelin receptor signaling by lipids. Nat. Commun. *12*, 3938. https://doi.org/10.1038/s41467-021-23756-y.

21. Forsén, S., Drakenberg, T., and Wennerström, H. (1987). NMR studies of ion binding in biological systems. Q. Rev. Biophys. *19*, 83–114. https://doi.org/10.1017/s0033583500004030.

22. Vickery, O.N., Carvalheda, C.A., Zaidi, S.A., Pisliakov, A.V., Katritch, V., and Zachariae, U. (2018). Intracellular transfer of Na(+) in an active-state G-protein-coupled receptor. Structure *26*, 171–180.e2. https://doi.org/10.1016/j.str.2017.11.013.

23. Leyris, J.-P., Roux, T., Trinquet, E., Verdié, P., Fehrentz, J.-A., Oueslati, N., Douzon, S., Bourrier, E., Lamarque, L., Gagne, D., et al. (2011). Homogeneous time-resolved fluorescence-based assay to screen for ligands targeting the growth hormone secretagogue receptor type 1a. Anal. Biochem. *408*, 253–262. https://doi.org/10.1016/j.ab.2010.09.030.

24. Damian, M., Marie, J., Leyris, J.-P., Fehrentz, J.-A., Verdié, P., Martinez, J., Banères, J.L., and Mary, S. (2012). High constitutive activity is an intrinsic feature of ghrelin receptor protein: a study with a functional monomeric GHS-R1a receptor reconstituted in lipid discs. J. Biol. Chem. *287*, 3630–3641. https://doi.org/10.1074/jbc.M111.288324.

25. Humphrey, W., Dalke, A., and Schulten, K. (1996). VMD: visual molecular dynamics. J. Mol. Graph. *14*, 33–38. https://doi.org/10.1016/0263-7855(96)00018-5.

26. Grant, B.J., Rodrigues, A.P.C., ElSawy, K.M., McCammon, J.A., and Caves, L.S.D. (2006). Bio3d: an R package for the comparative analysis of protein structures. Bioinformatics *22*, 2695–2696. https://doi.org/10.1093/bioinformatics/btl461.

27. Abraham, M.J., Murtola, T., Schulz, R., Páll, S., Smith, J.C., Hess, B., and Lindahl, E. (2015). GROMACS: high performance molecular simulations through multi-level parallelism from laptops to supercomputers. SoftwareX *1-2*, 19–25. https://doi.org/10.1016/j.softx.2015.06.001.

28. Woessner, D.E. (2001). NMR relaxation of spin-(3)/(2) nuclei: effects of structure, order, and dynamics in aqueous heterogeneous systems. Concepts Magn. Reson. *13*, 294–325. https://doi.org/10.1002/cmr.1015.

29. Czaplicki, J., Cornélissen, G., and Halberg, F. (2006). GOSA, a simulated annealing-based program for global optimization of nonlinear problems, also reveals transyears. J. Appl. Biomed. *4*, 87–94. https://doi.org/10.32725/jab.2006.008.

30. Filippov, A., Orädd, G., and Lindblom, G. (2009). Effect of NaCl and CaCl(2) on the lateral diffusion of zwitterionic and anionic lipids in bilayers. Chem. Phys. Lipids *159*, 81–87. https://doi.org/10.1016/j.chemphyslip.2009.03.007.

31. Lindblom, G., Rilfors, L., Hauksson, J.B., Brentel, I., Sjölund, M., and Bergenståhl, B. (1991). Effect of head-group structure and counterion condensation on phase equilibria in anionic phospholipid-water systems studied by 2H, 23Na, and 31P NMR and X-ray diffraction. Biochemistry *30*, 10938–10948. https://doi.org/10.1021/bi00109a019.

32. Maity, P., Saha, B., Kumar, G.S., and Karmakar, S. (2016). Binding of monovalent alkali metal ions with negatively charged phospholipid membranes. Biochim. Biophys. Acta *1858*, 706–714. https://doi.org/10.1016/j.bbamem.2016.01.012.

33. Friedman, R. (2018). Membrane-ion interactions. J. Membr. Biol. *251*, 453–460. https://doi.org/10.1007/s00232-017-0010-y.

34. Vrbka, L., Vondrásek, J., Jagoda-Cwiklik, B., Vácha, R., and Jungwirth, P. (2006). Quantification and rationalization of the higher affinity of sodium over potassium to protein surfaces. Proc. Natl. Acad. Sci. USA *103*, 15440–15444. https://doi.org/10.1073/pnas.0606959103.

35. Huang, J., Rauscher, S., Nawrocki, G., Ran, T., Feig, M., de Groot, B.L., Grubmüller, H., and MacKerell, A.D., Jr. (2017). CHARMM36m: an improved force field for folded and intrinsically disordered proteins. Nat. Methods *14*, 71–73. https://doi.org/10.1038/nmeth.4067.

36. Webb, B., and Sali, A. (2016). Comparative protein structure modeling using MODELLER. Curr. Protoc. Protein Sci. *86*. https://doi.org/10.1002/cpps.20.

37. Jo, S., Kim, T., Iyer, V.G., and Im, W. (2008). CHARMM-GUI: a web-based graphical user interface for CHARMM. J. Comput. Chem. *29*, 1859–1865. https://doi.org/10.1002/jcc.20945.

38. Berendsen, H.J.C., Postma, J.P.M., Vangunsteren, W.F., Dinola, A., and Haak, J.R. (1984). Molecular-dynamics with coupling to an external bath. J. Chem. Phys. *81*, 3684–3690. https://doi.org/10.1063/1.448118.

39. Jo, S., Kim, T., and Im, W. (2007). Automated builder and database of protein/membrane complexes for molecular dynamics simulations. PLoS One *2*, e880. https://doi.org/10.1371/journal.pone.0000880.

40. Essmann, U., Perera, L., Berkowitz, M.L., Darden, T., Lee, H., and Pedersen, L.G. (1995). A smooth particle mesh Ewald method. J. Chem. Phys. *103*, 8577–8593. https://doi.org/10.1063/1.470117.

41. Nosé, S., and Klein, M.L. (1983). Constant pressure molecular-dynamics for molecular-systems. Mol. Phys. *50*, 1055–1076. https://doi.org/10.1080/00268978300102851.

42. Hoover, W.G. (1985). Canonical dynamics - equilibrium phase-space distributions. Phys. Rev. A Gen. Phys. *31*, 1695–1697. https://doi.org/10.1103/PhysRevA.31.1695.

43. Parrinello, M., and Rahman, A. (1981). Polymorphic transitions in single-crystals - a new molecular-dynamics method. J. Appl. Phys. *52*, 7182–7190. https://doi.org/10.1063/1.328693.

44. Yin, J., Chen, K.Y.M., Clark, M.J., Hijazi, M., Kumari, P., Bai, X.C., Sunahara, R.K., Barth, P., and Rosenbaum, D.M. (2020). Structure of a D2 dopamine receptor-G-protein complex in a lipid membrane. Nature *584*, 125–129. https://doi.org/10.1038/s41586-020-2379-5.

STAR★METHODS

KEY RESOURCES TABLE

REAGENT or RESOURCE	SOURCE	IDENTIFIER
Bacterial and virus strains		
Escherichia coli BL21(DE3)	Sigma-Aldrich	cat # 69450-4
Chemicals, peptides, and recombinant proteins		
Thrombin	Sigma Aldrich	cat #T7009
Fluorescent ghrelin	Leyris et al., 2011[23]	N/A
ampicillin	Sigma Aldrich	cat # A9518
IPTG	Sigma Aldrich	cat #I6758
amphipol A8-35	Anatrace	cat # A835 100 MG
β-DDM	Anatrace	cat #D310
cholesteryl-hemisuccinate	Anatrace	cat # CH210
POPC	Avanti Polar Lipids	cat # 850457C
POPG	Avanti Polar Lipids	cat # 840457C
Biobeads SM2	BIO-RAD	cat # 1528920
NiNTA Superflow	Qiagen	cat # 30430
superdex S200 increase 10x300 GL	Cytiva	cat # 28990944
Critical commercial assays		
GTPase-GloTM assay	Promega	cat #V7681
Deposited data		
MD simulations	This manuscript	https://mycore.core-cloud.net/index.php/s/cRUxvdjvCn4O5I6
Recombinant DNA		
pMSP1E3D1	Addgene	cat # 20066
pET21a-alpha5-GHSR (transfected construct; *Homo sapiens*)	Damian et al., 2012[24]	N/A
Software and algorithms		
Prism	GraphPad	version 8.4.3
VMD	Humphrey et al., 1996[25]	N/A
Bio3	Grant et al., 2006[26]	N/A
Pymol 2.4.1.	Schrodinger LLC	http://pymol.org/2/#opensource
Gromacs 2020.3	Abraham et al., 2015[27]	N/A

RESOURCE AVAILABILITY

Lead contact

Further information and requests for resources and reagents should be directed to the lead contact, Jean-Louis Banères (jean-louis.baneres@umontpellier.fr).

Materials availability

This study did not generate new unique reagents.

Data and code availability

- The MD simulation data have been deposited at https://mycore.core-cloud.net/index.php/s/cRUxvdjvCn4O5I6 and are publicly available. All other data reported in this paper will be shared by the lead contact upon request.
- This paper does not report original code.
- Any additional information required to reanalyze the data reported in this paper is available from the lead contact upon request.

EXPERIMENTAL MODEL AND SUBJECT DETAILS

This study used the following cell line: *E. coli* BL21(DE3) (Sigma-Aldrich).

METHOD DETAILS

Production of GHSR

Human GHSR and its mutants were expressed in *E. coli* BL21(DE3) inclusion bodies as a fusion protein with the α_5 integrin fragment.[24] After thrombin cleavage, the receptor was folded in amphipol A8-35 from an SDS-unfolded state and then A8-35 was exchanged to n-Dodecyl-β-D-Maltopyranoside (β-DDM).[24] For reconstitution into nanodiscs, the His-tagged receptor in 25 mM HEPES, 100 mM NaCl, 2 mM β-DDM was first batch-bound onto a pre-equilibrated Ni-NTA superflow resin at a protein-to-resin ratio of about 0.2 mg of receptor per mL of slurry. The slurry was then mixed with 10 μM of JMV3011, and with MSP1E3D1(−) and a POPC:POPG (4:1 molar ratio) mixture at a 0.1:1:75 receptor:MSP:lipid ratio, with the receptor still immobilized on the Ni-NTA matrix. After 1h incubation at 4°C, polystyrene beads (Bio-Beads SM-2) were added at an 80% (w/v) ratio and incubated under smooth stirring for 4 hours at 4°C. The resin was then extensively washed with a 50 mM Tris-HCl pH 8, 150 mM NaCl, 1 μM JMV3011 buffer and the His-tagged receptor eluted with the same buffer containing 200 mM imidazole. After extensive dialysis in a 25 mM HEPES, 150 mM NaCl, 0.5 mM EDTA, pH 7.5 buffer, active receptor fractions were purified using affinity chromatography. To this end, the receptor in lipid discs was loaded on a streptavidin-agarose column where biotinylated JMV2959 had been bound. After washing with 25 mM Tris-HCl, 150 mM NaCl, pH 7.4, the bound proteins were recovered by washing the column with the same buffer containing 1 mM of the low affinity JMV4183 antagonist. The latter was removed through extensive dialysis against a 100 mM TEA-Cl, pH 7.4 buffer. Homogeneous fractions of GHSR-containing discs were finally obtained through a size-exclusion chromatography step on an S200 increase column (10/300 GL) using the same 100 mM TEA-Cl, pH 7.4 buffer as the eluent. Using ^{23}Na NMR, we could estimate the amount of residual sodium in the TEA buffer by plotting the intensity of the sodium peak as a function of NaCl concentration. The value thus obtained was below 1 mM. Taking into account an affinity value of GHSR for sodium ions in the 40 mM range, this amount of Na should not dramatically impact our observations on the effect of sodium on GHSR functioning.

^{23}Na-NMR measurements

^{23}Na-NMR spectra were acquired on a 500-MHz Bruker Avance spectrometer, using a 5 mm broadband probe, with deuterium lock, that was tuned to the ^{23}Na frequency of 132.256 MHz. The temperature of the sample was maintained at 278K ± 0.1 K with a Bruker variable temperature unit and calibrated from a methanol reference sample. The 200 μL samples were prepared in 3 mm NMR tubes. The ^{23}Na $\pi/2$ pulses had a length of 13 μs and were applied at the exact sodium resonance frequency. The dwell time was 49 μs, and 8k data point were acquired, for a total acquisition time of 400 ms (*i.e.*, above $10xT_1$). An additional inter-scan delay was set to 500 ms for the T_1 measurements, in order to allow for a complete recovery of magnetization. The number of scans was 6144 for the lower sodium concentration (3 mM), giving a signal to noise ratio superior to 100. For higher sodium concentrations, the number of scans was reduced while maintaining the signal to noise ratio to 200 (for NaCl = 10 mM) or higher. For each sample, a 1D ^{23}Na spectrum was recorded and the absolute signal intensity was determined in order to accurately correct sodium concentration by fitting expected and observed intensities. Indeed, in some cases, residual sodium from the buffers may modify the smaller sodium concentrations. T_1 relaxation times were measured using a standard inversion recovery pulse sequence with a composite π pulse $(\pi/2)_x - \pi_y - (\pi/2)_x$. Ten relaxation delays were acquired: 10 μs and 1, 2, 4, 10, 20, 30, 50, 100 and 500 ms. T_2 relaxations times were measured with standard CPMG experiments at 500 Hz CPMG frequency. Ten relaxation delays were acquired: 6.5 μs and 4, 8, 12, 16, 20, 28, 36, 44 and 60 ms. The total experimental time for one titration (1D spectrum, T_1 and T_2 measurement at five sodium concentrations) was 24 hours. The relaxation decays were fitted by mono-exponentials using the Bruker topspin relaxation module. Relative standard errors ($\delta T/T$) for the fittings of T_{1s} and T_{2s} were lower than ±0.05% in all cases. Based on three independent measurements, the relative standard deviation on T_1, T_2, R_1 and R_2 was estimated to ±0.3%. For every binding curve analyses, T_1 and T_2 were measured at five NaCl concentrations: 3, 10, 30, 100 and 400 mM. These concentrations were chosen to encompass the expected K_d value of about 40 mM, based on previous data with A_2AR.[10] The lower limit of 3 mM was chosen for sensitivity reasons and the higher limit of 400 mM because we observed an increasing role of non-specific binding above 500 mM and because very high salt concentrations may have an adverse effect on the receptor and/or nanodiscs stability. After measuring the 3 mM concentration point, the sodium concentration was increased by adding a few microliters of NaCl buffer solution prepared with the same H_2O/D_2O ratio of 91/9. This was important since the D_2O proportion affects viscosity, and thus T_1 and T_2, in a significant manner. The receptor concentration was recalculated for each sample by considering the dilution factor. Although R_1 and R_2 measurement are quite accurate, it may be noted that the uncertainty on K_d remains substantial (25%). This is because two unknown parameters in addition to the K_d have to be fitted (R_{ns} and k, see below), and because the binding curve has a very simple shape. Adding more concentration points would only slightly improve the accuracy at the expense of the experimental time; the five chosen sodium concentrations thus appeared to be an optimum compromise.

Theory of sodium relaxation

The theory of sodium quadrupolar relaxation is thoroughly described in the review of D. Woessner,[28] and briefly summarized here. The NMR relaxation times of spin 3/2 nuclei are determined mainly by the interaction between the nuclear electric quadrupole moment eQ and the electric field gradients at the nucleus. The longitudinal (R_1) and transverse (R_2) relaxation rates are given by the following expressions:

$$R_1 = \left(\frac{1}{5}\right) \cdot A \cdot (J_1(\omega_0) + 4J_2(2\omega_0))$$

$$R_2 = \left(\frac{1}{10}\right) \cdot A \cdot (3J_0(0) + 5J_1(\omega_0) + 2J_2(2\omega_0))$$

where $J_n(\omega_0) = \tau_c/(1 + n^2\omega_0{}^2\tau_c{}^2)$ are the spectral density function values at the sodium Larmor frequency ω_0; τ_c is the correlation time that gives the time scale of the fluctuations in the quadrupole interaction due to rotational diffusion of sodium ions, and $A = 2.\sigma^2$, with σ^2 the mean square of the angular quadrupole frequency ($A_f = 4.8\ 10^{12}\ s^{-2}$ for free sodium in water solution,[28] $\omega_0 = 8.31\ 10^8$ rd/s).

Sodium ions exchange rapidly between a bound and a free state, so that the relaxation rates are weighted averages between their value in the free (f) and bound (b) forms. Hence:

$$R = x_f R_f + x_b R_b,$$

where x_f and x_b are the free- and bound-sodium fractions, and R_f and R_b are the free and bound relaxation rates.

For free sodium in solution, $\tau_c \simeq 4$ ps,[28] $\omega_0\tau_c << 1$, $J_n(\omega_0) \simeq \tau_c$, so that

$$R_1 = R_2 \simeq A_f \cdot \tau_c, \text{thus}$$

$$R_1 = x_f \cdot A_f \cdot \tau_f + \left(\frac{1}{5}\right) \cdot x_b \cdot A_b \cdot (J_{1b}(\omega_0) + 4J_{2b}(2\omega_0))$$

$$R_2 = x_f \cdot A_f \cdot \tau_f + \left(\frac{1}{10}\right) \cdot x_b \cdot A_b \cdot (3J_{0b}(0) + 5J_{1b}(\omega_0) + 2J_{2b}(2\omega_0))$$

Note that the A value may be different in the free and bound states due to different coordination of sodium ions, and thus different quadrupole moments.

Measuring both R_1 and R_2 to calculate the difference $R_2 - R_1$ allows us to eliminate the contribution from the free state, which may vary over the course of sodium titrations due to changes in viscosity (Figure 1 in Woessner[28]).

$$R_2 - R_1 = x_b \cdot A_b \left[\left(\frac{3}{10}\right) \cdot (J_{0b}(0) + J_{1b}(\omega_0) - 2J_{2b}(2\omega_0))\right] = k \cdot x_b$$

This expression shows that R_2 - R_1 is proportional to the bound fraction x_b, so that the sodium titration of a receptor allows us to extract the binding constant, even though A_b and τ_b, and thus the proportionality constant $k \simeq (3/10).A_b.\tau_b$, are not known.

In practice, the receptor (typically at 10 μM) is titrated with increasing concentrations of sodium (from 3 mM to 400 mM), and the sodium R_2 and R_1 relaxation rates are measured for each sodium concentration. The resulting R_2 - R_1 = f([Na^+]) curve are then fitted by a single site binding equation:

$$Na^+ + R \rightleftarrows (Na^+\text{-}R)$$

$$R_2 - R_1 = k \cdot \frac{\frac{1}{2}\left((K_d + x + c_0) - \left[(K_d + x + c_0)^2 - 4 \cdot x \cdot c_0\right]^{1/2}\right)}{x} - \frac{1}{2}\left((K_d + x + c_0) - \left[(K_d + x + c_0)^2 - 4 \cdot x \cdot c_0\right]^{1/2}\right) + R_{ns}$$

where K_d is the sodium dissociation constant, c_0 the known total receptor concentration and x the total sodium concentration. The term R_{ns} is added to account for the contribution from non-specific binding to the relaxation rates (binding to any non-saturable site such as to the NMR tube walls). In the present work, the curves R_2-R_1 versus x were fitted with this equation using an in house software, GOSA,[29] with k, K_d and R_{ns} as adjustable parameters. It allowed to extract a reliable K_d value, as long as this value lied within the sodium concentrations range of the titration (typically for K_d values comprised between 10 and 100 mM).

Sodium non-specific binding

Although one can reproducibly and accurately measure R_1 and R_2, a major concern is the possible contribution of non-specific binding to the relaxation rates. Typical values for the binding constant of sodium to neutral lipid bilayers are around 1 M^{-1}.[30–33] However, one should also consider Gouy-Chapman electrostatic accumulation at the surface of negatively charged membranes. Maity et al.[32] found that, while having an *intrinsic* affinity around 1 M^{-1}, sodium ions significantly accumulate at the surface of 4/1 POPC-POPG bilayers at low ionic strength (200 mM for 10 mM in the bulk), giving an apparent K_d of 50 mM. This value closely approaches the ones that have been reported for GPCR sodium binding sites. Furthermore, such a binding may occur with negatively charged lipid nanodiscs, as those used in the present work, or with the detergent micelles that are typically used to solubilize GPCRs (DDM-CHS or LMNG-CHS), as CHS (cholesterol hemi-succinate) is negatively charged at neutral pH.

We first investigated the apparent binding of sodium in the presence of DDM-CHS micelles and observed a drastic increase in R_2 at low sodium concentration (Figure S1). It highlighted an important contribution from interactions with the surface of the micelles. This curve could not be fitted by a single site binding isotherm because Gouy-Chapman accumulation is largely responsible for sodium binding. This result was further confirmed by adding 150 mM of KCl to the solution, which completely abolished the changes in R_2 through an increase of the ionic strength of the solution (Figure S1A). The addition of 10 mM $MgCl_2$ produced a similar result.

We then aimed to suppress this non-specific contribution to reliably measure sodium binding to GHSR in lipid nanodiscs containing negatively charged lipids. The obvious way is to increase the ionic strength of the buffer. Although 150 mM KCl could be an option, we observed that potassium at high concentration partially competes with sodium binding to GHSR. Therefore, as stated in the result section, we chose to use tri-ethyl ammonium (buffer with 100 mM HEPES-TEA pH 7.4 and H_2O/D_20 91/9). Using ^{23}Na NMR, we could estimate the amount of residual sodium in the TEA buffer by plotting the intensity of the sodium peak as a function of NaCl concentration. The value thus obtained was below 1 mM. Under such conditions, we were able to minimize the effect of binding to the empty nanodiscs to a negligeable level. Namely, for 10 mM NaCl, we obtained R_2-R_1 = 0.3 Hz (R_1 = 28.2 Hz, R_2 = 28.5 Hz) with 7.1 μM empty nanodiscs, in contrast to R_2-R_1 = 8.6 Hz (R_1 = 28.7 Hz, R_2 = 37.3 Hz) with ∼10 μM GHSR-containing nanodiscs.

The receptor itself may display patches of negatively charged amino-acids such as aspartates and glutamates at its surface. Binding of sodium to these residues was also described to occur with an affinity value in the M^{-1} range.[34] In order to check whether this could also contribute to non-specific binding and affect sodium relaxation, we measured sodium relaxation in the presence of bovine serum albumin (BSA) (Figure S1C). This 66 kDa protein is highly negatively charged (pI = 4.7), with an excess of 30–40 negative charges at neutral pH. Surprisingly, we observed that BSA had little effect on sodium R_2 relaxation rates. It is possible that the significant increase in R2 does not result from electrostatic accumulation only but also involves the simultaneous coordination of sodium ions by several carboxylates. This may occur on a micelle surface more efficiently than with BSA because the CHS carboxylates are free to move laterally and to cluster around sodium ions, thus creating an ion coordination site.

Molecular dynamics

The ghrelin receptor was retrieved from its available X-ray structure describing an antagonist-bound state (PDB: 6KO5)[13] and submitted to MD simulations using GROMACS v.2020.4[27] under the CHARMM36m force field.[35] The native sequence of GHSR was used, replacing K130$^{3.39}$ and Q188 in the structure with a threonine and an asparagine, respectively. The missing segment G293-I300$^{7.30}$ (EL3) was built with MODELLER v9.19[36] and the final GHSR model was chosen by selecting the one with the best DOPE score among 100 models generated. The system was built with the CHARMM-GUI web-server[37] by embedding the receptor in a membrane of 80x80 Å^2 composed of POPC and POPG in percentages of 80 and 20, respectively. The system was solvated, neutralized and then NaCl was added until reaching a concentration of 0.15 M. Equilibration was performed in an NVT ensemble followed by an NPT ensemble at 300 K and 1 bar using the Berendsen weak-coupling thermostat and barostat.[38] The membrane was submitted to a gradual decreasing position restraints protocol until reaching zero, according to the CHARMM-GUI protocol.[39] During these steps, the backbone and sidechain atoms of GHSR were restrained with a force constant of 1000 and 500 kJ.mol^{-1}.nm^{-2}, respectively. Then three further steps of 1 ns each were added to reduce these position restraints until zero, while the lipids were free to accommodate around the receptor. Non-bonded interactions were calculated up to 10 Å with a switching-force function acting in the range of 10–12 Å. Long-range electrostatic interactions were treated within a 12 Å cut-off with the particle-mesh Ewald (PME) method.[40] The production phase was run in the NPT ensemble over 1 μs with a time-step of 2 fs using the Nose-Hoover thermostat[41,42] and Parrinello-Rahman barostat.[43] Five independent simulations were run to verify reproducibility. Data were collected every 50 ps. Analyses were performed using homemade scripts implemented in VMD.[25] The same protocol was employed for the simulations of the dopamine D2 receptor (PDB: 6VMS),[44] removing all other proteins or small molecules and adding C443 lipidation prior to build the system. Molecular dynamics data are freely available at https://mycore.core-cloud.net/index.php/s/cRUxvdjvCn4O5l6.

Functional assays

Ligand-binding assays were performed using fluorescence energy transfer with the purified receptor labeled at its N-terminus with Lumi-4 Tb NHS and a dy647-labeled ghrelin peptide.[24] After a 30-minute incubation of the receptor with different labeled ghrelin concentrations at 15°C, fluorescence emission spectra were recorded at the same temperature between 400 and 600 nm (Cary Eclipse spectrofluorimeter, Varian) with excitation at 346 or 488 nm. For GTP turnover assays, the receptor (200 nM) was first incubated with the isolated G protein (500 nM) and, when applicable, the ligand (10 μM) for 30 minutes in a 25 mM HEPES, 100 mM NaCl, 5 mM $MgCl_2$, pH 7.5 buffer containing either 250 mM NaCl or 250 mM TEA-Cl. GTP turnover was then started by adding GTP (1 μM)

and the remaining amount was assessed after 40 minutes incubation at room temperature using the GTP-Glo assay (Promega).[20]

Bimane labeling and fluorescence experiments

Monobromobimane was introduced in a cysmin mutant of GHSR with a single reactive cysteine at position 255$^{6.27}$. The receptor was first incubated in the dark with a 1.5 molar excess in monobromobimane at 4°C for 16 h.[20] Unreacted dye was removed by extensive dialysis against a buffer 25 mM HEPES, 0.5 mM EDTA, pH 7.5 containing either 250 mM NaCl or 250 mM TEA-Cl. Fluorescence experiments were performed on a Cary Eclipse fluorimeter (Varian) with a pulsed Xe-Lamp. For each scan, the receptor concentration was 5 μM, λ_{exc} was set at 380 nm, the excitation and emission bandpass set at 5 nm, and emission measured between 410 nm and 520 nm. All experiments were performed at 20°C. Fluorescence intensity was corrected for any dilution effect and normalized to the emission of the apo receptor in the presence of sodium.

QUANTIFICATION AND STATISTICAL ANALYSIS

As stated in the legends of the corresponding figures, data are presented as mean ± SD of three experiments. All analysis steps, including the sample size, were decided before looking at the data. No data was removed from the analysis.